

# Photoassisted “Gate-Lock” Fluorescence “Turn-on” in a New Schiff Base and Coordination Ability of *E–Z* Isomers

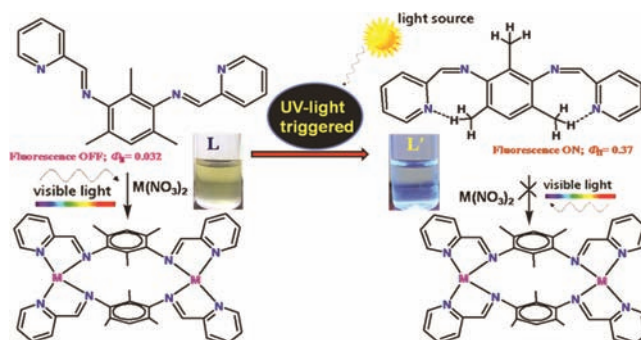
Rampal Pandey,<sup>†</sup> Rakesh Kumar Gupta,<sup>†</sup> Pei-Zhou Li,<sup>‡</sup> Qiang Xu,<sup>‡</sup> Arvind Misra,<sup>†</sup> and Daya Shankar Pandey<sup>\*,†</sup>

Department of Chemistry, Faculty of Science, Banaras Hindu University, Varanasi -221 005 (U.P.), India, and National Institute of Advanced Industrial Science and Technology (AIST), 1-8-31 Midorigaoka, Ikeda, Osaka 563-8577, Japan

dspbhu@bhu.ac.in

Received December 1, 2011

## ABSTRACT



Rapid photoresponse (1.0–8.0 min) through fluorescence “turn-on” signaling displayed by a novel Schiff base (L) creating “gate lock” via intramolecular C–H···N interaction in photoisomerized product (L') has been described. Coordination chemistry of pre- and postirradiated species demonstrated a drastic change in the reactivity which has been supported by NMR, HRMS, UV–vis, emission, electrochemical, and complexation studies.

Light-regulatable fluorescent compounds that undergo structural, conformational, and dynamic changes triggered by light excitation find wide applications as temporal probes.<sup>1</sup> The light-induced structural changes can be easily evaluated if they are directly related to a fluorescent readout.<sup>2</sup> Photoactivation of the compounds in biological systems frequently leads to fluorescence “turn-on” by release of fluorophores with reasonable photostability.<sup>3</sup> Considering their electrical and optical properties, some

chemical, biological, gas, and UV-light sensors have been developed.<sup>4</sup> Among these, UV-responsive compounds are in high demand because of their potential applications in diverse areas.<sup>5a,6</sup> Although “off–on” UV-light switches containing ZnO, CdS quantum dots/graphene, and a few retinal-linked Schiff bases have been reported, a selective and sensitive UV-light “off–on” switch based on a free Schiff base has not been described.<sup>5,7</sup>

Further, metallo-supramolecular entities, metallo-hosts, and related systems have received substantial interest owing to their potential application in various fields.<sup>8</sup> Creation of such a system is directed by the relative position of nitrogen atoms in bis-imine Schiff bases.<sup>9,10</sup> To our knowledge, Schiff bases derived from the condensation

(1) (a) Patterson, G. H.; Lippincott-Schwartz, J. *Science* **2002**, *297*, 1873. (b) Lee, H. M.; Larson, D. R.; Lawrence, D. S. *ACS Chem. Biol.* **2009**, *4*, 409. (c) Mayer, G.; Heckel, A. *Angew. Chem., Int. Ed.* **2006**, *45*, 4900. (d) Gröbner, G.; Burnett, I. J.; Glaubitz, C.; Choi, G.; Mason, A. J.; Watts, A. *Nature* **2000**, *405*, 810.

(2) (a) Gurskaya, N. G.; Verkhusha, V. V.; Shcheglov, A. S.; Staroverov, D. B.; Chepurnykh, T. V.; Fradkov, A. F.; Lukyanov, S.; Lukyanov, K. A. *Nat. Biotechnol.* **2006**, *24*, 461. (b) Masuda, S.; Hasegawa, K.; Ishii, A.; Ono, T.-A. *Biochemistry* **2004**, *43*, 5304.

(3) (a) Theriot, J. A.; Mitchison, T. J. *Nature* **1991**, *352*, 126. (b) Kobayashi, T.; Urano, Y.; Kamiya, M.; Ueno, T.; Kojima, H.; Nagano, T. *J. Am. Chem. Soc.* **2007**, *129*, 6696.

(4) (a) Wang, Z. L. *Adv. Mater.* **2003**, *15*, 432. (b) LaFratta, C. N.; Walt, D. R. *Chem. Rev.* **2008**, *108*, 614.

(5) (a) Fang, X.; Bando, Y.; Liao, M.; Gautam, U. K.; Zhi, C.; Dierre, B.; Liu, B.; Zhai, T.; Sekiguchi, T.; Koide, Y.; Golberg, D. *Adv. Mater.* **2009**, *21*, 2034.

(6) Spudich, J. L.; Yang, C.-S.; Jung, K.-H.; Spudich, E. N. *Annu. Rev. Cell Dev. Biol.* **2000**, *16*, 365.

(7) Nielsen, I. B.; Petersen, M. A.; Lammich, L.; Nielsen, M. B.; Andersen, L. H. *J. Phys. Chem. A* **2006**, *110*, 12592.

of phenylene-1,3-diamine with pyridyl-*n*-carboxaldehydes ( $n = 2/3/4$ , Scheme S1, Supporting Information) have not been reported.<sup>9,10</sup> The objective of designing a selective and sensitive photoresponsive compound can be achieved by developing a conjugated  $\pi$ -electron system, which can assume a more stable configuration by acquiring an appropriate amount of energy. Based on our earlier results and those from other groups,<sup>10,11</sup> through this contribution we describe a new Schiff base 2,4,6-trimethyl[*N,N'*-bis-(pyridin-2-ylmethylene)]benzene-1,3-diamine (**L**) which acts as photoswitch and is blind to visible light. The UV-triggered fluorescence enhancement via structural changes and coordination chemistry of both photoisomers has not been described to the best of our knowledge.

Figure 1 summarizes the synthetic strategy for preparation of **L** and its response toward UV-light and metal ions. Schiff base **L** was synthesized by condensation of pyridine-2-carboxaldehyde with 2,4,6-trimethylbenzene-1,3-diamine (2: 1) in benzene (Scheme S1, Supporting Information) in reasonably good yield (83%).

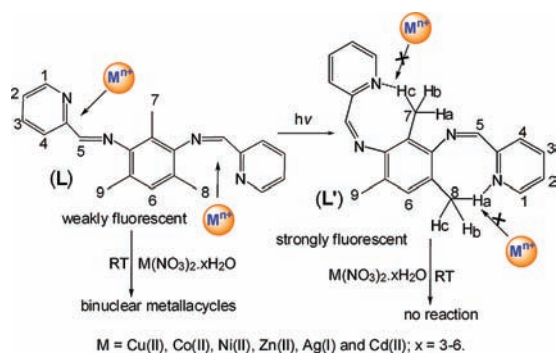


**Figure 1.** Structures of **L** and **L'** and approach of metal ions toward the coordination sites of both isomers.

Details about the synthesis of **L/L'**, metallacycles 1–6, and their characterization data is given in the Supporting Information. The characterization of **L** has been achieved by satisfactory elemental analyses, FT-IR, NMR [<sup>1</sup>H, <sup>13</sup>C, 2D COSY (<sup>1</sup>H–<sup>1</sup>H, <sup>1</sup>H–<sup>13</sup>C), and DEPT (135°/90°)], UV–vis, fluorescence, and cyclic voltametric studies.

(8) (a) Lehn, J. M. *Supramolecular Chemistry: Concepts and Perspectives*; VCH: Weinheim, 1995; Chapter 9. (b) Lehn, J. M. *Science* **2002**, 295, 2400. (c) Yam, V. W. W.; Lo, K. K. W. *Chem. Soc. Rev.* **1999**, 28, 323. (d) Albrecht, M. *Chem. Rev.* **2001**, 101, 3457. (e) Nabeshima, T. *Coord. Chem. Rev.* **1996**, 148, 151. Fujita, M.; Tominaga, M.; Hori, A.; Therrien, B. *Acc. Chem. Res.* **2005**, 38, 371.

(9) (a) Nakasuka, N.; Kunimatsu, M.; Matsumura, K.; Tanaka, M. *Inorg. Chem.* **1985**, 24, 10. (b) Pardo, E.; Ruiz-García, R.; Lloret, F.; Julve, M.; Cano, J.; Pasàn, J.; Ruiz-Pérez, C.; Filali, Y.; Chamoreau Journaux, L.-M. Y. *Inorg. Chem.* **2007**, 46, 4504. (c) Halder, P.; Zangrando, E.; Paine, T. K. *Dalton Trans.* **2009**, 5386.

(10) (a) Pandey, R.; Kumar, P.; Singh, A. K.; Shahid, M.; Li, P.-Z.; Singh, S. K.; Xu, Q.; Misra, A.; Pandey, D. S. *Inorg. Chem.* **2011**, 50, 3189. (b) Lavalette, A.; Hamblin, J.; Marsh, A.; Haddleton, D. M.; Hannon, M. J. *Chem. Commun.* **2002**, 3040. (c) Lavalette, A.; Tuna, F.; Clarkson, G.; Alcock, N. W.; Hannon, M. J. *Chem. Commun.* **2003**, 2666.

(11) Koner, R. R.; Ray, M. *Inorg. Chem.* **2008**, 47, 9122.

In the <sup>1</sup>H NMR spectrum of **L**, *H1* and *H4* protons resonated as doublets at  $\delta$  8.72 and 8.29 ppm (Figure S1a, Supporting Information) while *H5* (–CH=N–) and *H6* as singlets at  $\delta$  8.35 and 6.98 ppm. The triplets at  $\delta$  7.84 and 7.40 ppm has been assigned to *H3* and *H2* proton resonances. Methyl protons of the central mesitylene ring resonated at  $\delta$  2.15 (*H8/H9*) and 1.99 ppm, (*H7*) suggesting symmetrical orientation of the molecule. The aromatic protons (*H1*–*H6*) of **L'** exhibited small upfield shift (Figure S2a, Supporting Information). However, the signals due to methyl protons displayed splitting and appeared at  $\sim\delta$  2.18–1.98 ppm (downfield shift) indicating some sort of interaction between methyl protons and pyridyl nitrogen (Figure 1). Further, 2D COSY and DEPT NMR spectra of **L'** exhibited enhanced H–H and C–H coupling and the presence of –CH<sub>2</sub> and –CH aliphatic protons (Figure S4 and S5, Supporting Information). On the basis of NMR spectral studies we conclude that the intramolecular C–H $\cdots$ N interactions are responsible for the splitting of methyl protons. Stacked <sup>1</sup>H NMR spectra also supported UV-light induced structural changes (Figure S3, Supporting Information). The presence of molecular ion peak at *m/z*, 329 in the HRMS of both **L** and **L'** with different fragmentation patterns strongly supported our scheme (Figure 2b and S6, Supporting Information).

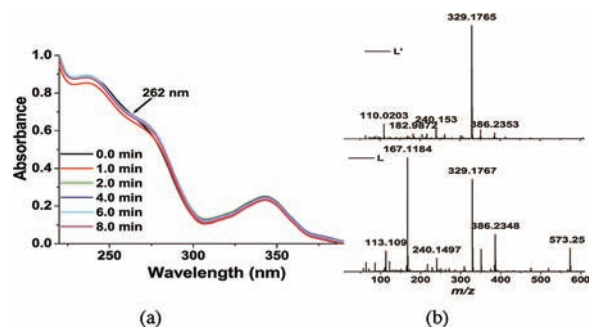


**Figure 2.** (a) Absorption spectra of **L** (5  $\mu$ M) and after UV irradiation. (b) HRMS spectra of **L** and **L'**.

UV–vis spectrum of **L** (10  $\mu$ M, Supporting Information) displayed transitions at 351, 271, and 238 nm assignable to  $n \rightarrow \pi^*$  and  $\pi \rightarrow \pi^*$  transitions (Table S2, Supporting Information). The absorption spectrum of **L** in methanol also exhibited a pattern analogous to that in H<sub>2</sub>O/MeCN system (Figure S7a, Supporting Information, inset). After UV irradiation (01 min, 365 nm; 5  $\mu$ M), the optical density of low energy band at 348 nm ( $\epsilon$ ,  $2.29 \times 10^4 \text{ M}^{-1} \text{ cm}^{-1}$ ) gradually increases while that for high energy band (271 nm,  $\epsilon$ ,  $6.20 \times 10^4 \text{ M}^{-1} \text{ cm}^{-1}$ ) decreases ( $\epsilon$ ,  $6.07 \times 10^4 \text{ M}^{-1} \text{ cm}^{-1}$ ) (Figure 2a). Notably, irradiation up to 2.0–8.0 min leads to a considerable change in the absorption spectra wherein low energy band showed hyperchromic shift ( $\epsilon$ ,  $2.51 \times 10^4 \text{ M}^{-1} \text{ cm}^{-1}$ ) and the high energy band a hypsochromic ( $\epsilon$ ,  $7.13 \times 10^4 \text{ M}^{-1} \text{ cm}^{-1}$ ) with red shift of  $\sim 3$ –5 nm. The isosbestic point at 275 nm (1.0 min exposure) disappeared upon increasing the

irradiation time (2.0–8.0 min) and a new one appeared at 264 nm. Narrow spectral alterations with two consecutive isosbestic points suggested the presence of more than one species.<sup>12</sup> Closer examination of the absorption spectra of **L** and **L'** (Figure 2) indicated some structural changes (i.e., orientation, geometry, etc.) retaining conjugation length. This can be rationalized by assuming the movement of pyridyl ring (*E,Z*) to form an eight membered cyclic ring (*Z,Z*) involving C–H···N hydrogen bonding between methyl protons and nitrogen lone pair.<sup>13</sup> The effect of metal ions were investigated under analogous conditions. Notably, interactions between **L'** and various metal ions led to insignificant changes (Figure S8, Supporting Information) suggesting **L** becomes inert toward the tested metal ions after UV exposure.

The Schiff base **L** fluoresces weakly at 430 nm ( $\lambda_{\text{exc}}$ , 350 nm;  $\Phi_{\text{fl}}$ , 0.032)<sup>14</sup> with a Stokes shift of  $5316 \text{ cm}^{-1}$  (Figure 3 and Table S2, Supporting Information), which may be attributed to photoinduced electron transfer process.<sup>14</sup> To examine the photostability of **L** fluorescence spectra of the same solution was acquired repeatedly with 1 min time interval which showed gradual increase in the relative emission intensity ( $\sim 91\%$ ). The light-induced fluorescence enhancement motivated us to scrutinize the cause of photoswitching ability. Therefore, fluorescence titrations were performed using **L** as a ‘host’ and light as a ‘guest’. After each excitation and proper mixing ( $\Delta t$ , 1.0 min) **L** showed gradual increase in the fluorescence intensity (Figure 3b) with insignificant change in the Stokes shift ( $53 \text{ cm}^{-1}$ ). The trend continued and attained saturation after 8.0 min (Figure 5, inset) with an increase in quantum yield by a factor of  $\sim 11$  ( $\Phi_{\text{fl}}$ , 0.377). Time versus intensity plot gave a sigmoid curve indicating two step structural changes (Figure 3b, inset). Fluorescence ‘turn-on’ without any significant change in Stokes shift suggested the possibility of structural changes rather than photocleavage. The interaction of solvent with **L** under influence of UV light cannot be ruled out; therefore, fluorescence behavior of **L** was investigated in MeOH, THF, DMF, DMSO, 1,4-dioxane,  $\text{CH}_2\text{Cl}_2$ , and  $\text{C}_6\text{H}_6$ . Notably, it exhibited an analogous pattern in the aforesaid solvents except a small decrease in relative intensity in  $\text{C}_6\text{H}_6$  (Figure S7b, Supporting Information).

To understand the reversibility of structural changes in the presence and absence of UV light, **L** (MeCN, 3 mL,  $100 \mu\text{M}$ ) was irradiated for different durations (10 min to 24 h, 365 nm) and monitored by emission spectral studies. The spectral features were similar for a sample irradiated for short (10 min) or long (24 h) time period suggesting that  $\sim 10$  min is sufficient for the conversion of **L** to **L'**. To

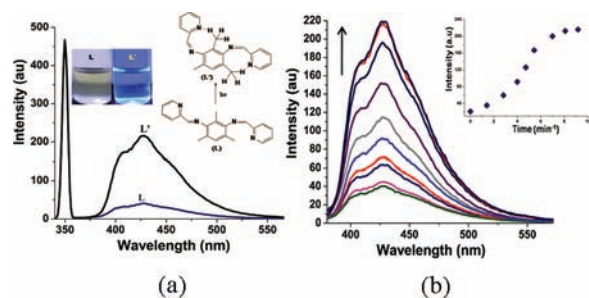


**Figure 3.** (a) Fluorescence spectra of **L** and **L'** (*c*,  $10 \mu\text{M}$ ;  $\lambda_{\text{exc}}$ , 350 nm). Inset shows structural and color changes upon irradiation. (b) Fluorescence titrations of **L** to **L'** (*c*,  $10 \mu\text{M}$ ). Inset shows fluorescence enhancement of **L** with respect to fraction of UV-light/min.

gain deep insight into wavelength triggered structural changes, **L** was irradiated at 254 nm. It showed behavior similar to that observed at 365 nm (Figure S9b, Supporting Information). Additionally, **L'** remains unchanged in dark (298 K,  $\text{CH}_2\text{Cl}_2$ , 24 h).

Based on our earlier findings,<sup>10</sup> the report by Ray et al.,<sup>11</sup> and NMR, HRMS, UV–vis, and fluorescence spectral data, we propose that light-induced structural changes in **L** retain the extent of conjugation and controlled by intramolecular C–H···N interactions.<sup>13</sup> The resulting eight-membered ring creates rigidity in the molecule which controls vibrational motion and in turn, fluorescence ‘turn-on’.<sup>15</sup> One can speculate that **L'** would be less reactive or inert toward metal ions. To affirm our postulation, nitrate salts of various metal ions were added to a solution of **L'** (Figure S9a, Supporting Information). It was observed that the fluorescence spectrum of **L'** remains unchanged indicating inertness of **L'** toward the metal ions. In contrast, such type of ligands show good coordination ability toward transition metals.<sup>10</sup>

Therefore, **L** and **L'** were treated with various metal ions in the absence of UV light in methanol at room temperature. Notably, **L** reacted readily with most of the metal nitrates and afforded binuclear metallacycles  $[\{\text{M}(\text{C}_{21}\text{H}_{20}\text{N}_4)\}_2]_2$  ( $\text{X}^-$ )<sub>*m*</sub> (**1–6**),  $[\text{Co}(\text{C}_{12}\text{H}_8\text{N}_3\text{O}_2)_2]\text{PF}_6 \cdot \text{H}_2\text{O}$  (**2b**), and  $[\{\text{Ni}(\text{C}_{21}\text{H}_{20}\text{N}_4)(\text{H}_2\text{O})_2\}_2](\text{NO}_3)_4$  (**3a**) (Scheme S2, Supporting Information), characterized by elemental analyses and spectral (FT-IR, NMR, absorption, and emission) and electrochemical studies (Figures S10–S12, Supporting Information). Structures of **1**, **2b**, **3a**, and **5** have been determined crystallographically (Figure 4 and Figure S13 and Table S1, Supporting Information). The crystal structure of **3a** exhibited a looped arrangement with double-stranded 12-membered metallamacrocyclic cation  $[\{\text{Ni}(\text{C}_{21}\text{H}_{24}\text{N}_4\text{O}_2)\}_2]^{4+}$  along with coordinated water molecules. In the cations of **3a** immediate coordination geometry about each Ni(II) is distorted octahedral with  $\text{NiN}_4\text{O}_2$  environment<sup>16</sup> and  $\text{N}_4\text{O}_2$

(12) Wöhri, A. B.; Katona, G.; Johansson, L. C.; Fritz, E.; Malmerberg, E.; Andersson, M.; Vincent, J.; Eklund, M.; Cammarata, M.; Wulff, M.; Davidsson, J.; Groenhof, G.; Neutze, R. *Science* **2010**, *328*, 630.

(13) (a) Lin, C.-W.; Chou, P.-T.; Liao, Y.-H.; Lin, Y.-C.; Chen C.-T.; Chen, Y.-C.; Lai, C.-H.; Chen, B.-S.; Liu, Y.-H.; Wang, C.-C.; Ho, M.-L. *Chem.–Eur. J.* **2010**, *16*, 3770. (b) Harlow, R. L.; Li, C.; Sammes, M. P. *J. Chem. Soc., Chem. Commun.* **1984**, 818.

(14) (a) Deda, M. L.; Ghedini, M.; Aiello, I.; Grisolia, A. *Chem. Lett.* **2004**, *33*, 1060. (b) Williams, N. J.; Gan, W.; Reibenspies, J. H.; Hancock, R. D. *Inorg. Chem.* **2009**, *48*, 1407.

(15) Grobner, G.; Burnett, I. J.; Glaubitz, C.; Choi, G.; James, A.; Watts, M. A. *Nature* **2000**, *405*, 810.

(16) Palacios, M. A.; Rodríguez-Diéguez, A.; Sironi, A.; Herrera, J. M.; Mota, A. J.; Cano, J.; Colacio, E. *Dalton Trans.* **2009**, 8538.

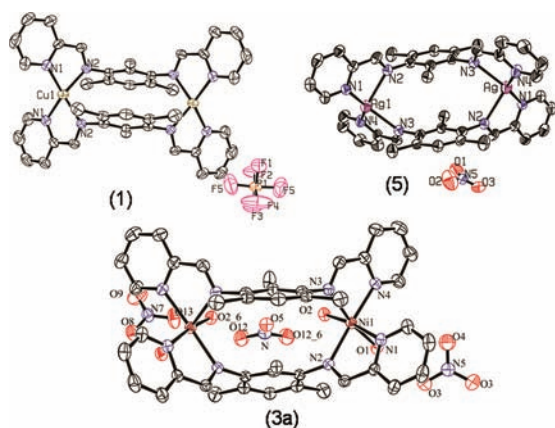


**Figure 4.** Crystal structures of **1**, **3a**, and **5** (30% thermal probability).

donor sites contains opposite ( $\Delta$ ,  $\Lambda$ ) chirality. It represents the first Ni(II) octahedral complex containing a Schiff base derived from substituted benzene-1,3-diamine.<sup>16</sup>

To have a clear correlation between **L** and corresponding metallacycles, the absorption and fluorescence behaviors of **1–6** were investigated (Figure 5 and Figure S14 and Table S2, Supporting Information). Among these, **1**, **2b**, **3a/3b** are nonfluorescent, while **4–6** displays strong fluorescence with significant Stokes shift relative to **L/L'** due to the chelation enhanced fluorescence (CHEF) process.<sup>17</sup>

On the other hand, the reaction between **L'** and metal nitrates under only visible light do not yield any complex at room temperature. Further, **L'** was extracted from the reaction mixture (96%) using dichloromethane. Marked difference in the reactivity of **L** and **L'** supported creation of a cyclic structure after UV irradiation, wherein the approach of metal is restricted by intramolecular C–H $\cdots$ N interactions “gate-lock” (Figure 1).<sup>13</sup>

Redox behavior of **L**, **L'** (Figure 6 and Table S2, Supporting Information) and metallacycles **1–6** (Figures S15–S22, Supporting Information) have been followed by cyclic voltammetry. The cyclic voltammogram of **L** displayed one irreversible wave at +1.63 V ( $E_{pa}$ ) in the anodic potential window. It has been tentatively assigned to oxidation of  $\pi$ -conjugated Schiff base (HOMO) to mono cationic (HOMO<sup>+</sup>) species.<sup>18</sup> The quasi-reversible waves at  $E_{pc}$  –1.38 and –1.97 V may be assigned to ligand based reductions.<sup>18</sup> Conversely, **L'** displayed an oxidative wave at +1.72 V and two quasi-reversible reductions –1.45, and –2.43 V. High positive and negative  $E_{1/2}$  values for **L'** are consistent with its stabilization relative to **L**. The observation is consistent with the conclusions drawn from optical studies.

Light induced *E–Z* isomerization in **L** and the presence of C–H $\cdots$ N interactions in **L'** has further been supported

(17) Burdette, S. C.; Lippard, S. J. *Coord. Chem. Rev.* **2001**, 216–217, 333.

(18) Bu, X. H.; Liu, H.; Du, M.; Wong, K. M. C.; Yam, V. W. W.; Shionoya, M. *Inorg. Chem.* **2001**, 40, 4143.

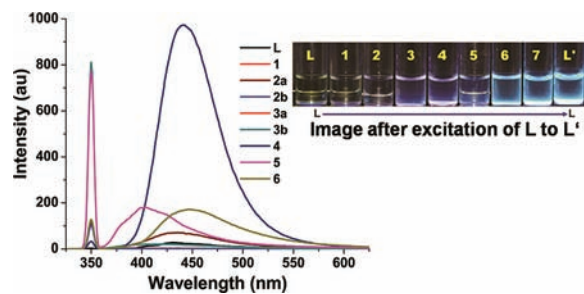


**Figure 5.** Fluorescence spectra of **1–6** (*c*, 10  $\mu$ M; H<sub>2</sub>O/MeCN, 7: 3). Inset shows fluorescence enhancements from **L** to **L'**.

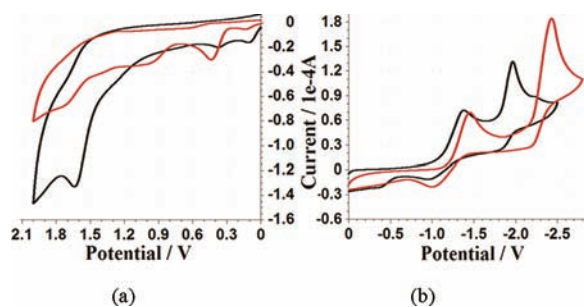


**Figure 6.** Cyclic voltammograms of **L** (black) and **L'** (red) in H<sub>2</sub>O/MeCN (7:3) in anodic (a) and cathodic (b) windows.

by comparing optical properties of **L**, **L'** and model system **L1**. The UV–vis spectra of **L1** exhibited changes due to *E–Z* isomerization, while fluorescence spectra remains unaltered upon UV-irradiation (Figure S23, Supporting Information).

Through this work we have presented a new Schiff base **L** exhibiting UV-triggered fluorescence ‘turn-on’ due to *E–Z* structural changes controlled by intramolecular C–H $\cdots$ N interactions leading to a gate-lock for metal ion coordination. Unambiguous support has been provided by NMR, HRMS, UV–vis, emission, and electrochemical studies and complexation behavior. Both **L** and **L'** are stable under visible light and exhibit marked difference in the reactivity toward various metal ions.

**Acknowledgment.** Thanks are due to the Department of Science and Technology (DST) and the Council of Scientific and Industrial Research (CSIR), New Delhi, India, for providing financial assistance through Schemes SR/S1/IC-15/2006 and 9/13(288)/2010-EMR-I.

**Supporting Information Available.** Schemes, NMR spectra, ORTEP view, optical plots, cyclic voltammograms, and tables. This material is available free of charge via the Internet at <http://pubs.acs.org>.